Journal of Energy Technology & Environment
www.nipes.org

System Dynamics And Performance Prediction Of A Wind-Powered Acoustic Bird Deterrent System

Onochojah Ufuoma*, Egbuchulam Ekenna, Onyiah Maxwell and Nwoke Collins
Projects Development Institute (PRODA), Enugu
Corresponding Author*: ufuomawilfred3@gmail.com

Article information

Article History
Received 24 September 2025
Revised 10 October 2025
Accepted 20 October 2025
Available online 02 December 2025

Keywords:
Wind-powered deterrents, Acoustic bird repellent, Blade Element Momentum (BEM) theory, System modeling, MATLAB/Simulink

https://doi.org/10.37933/jete/7.4.2025.2570

https://nipesjournals.org.ng

Abstract

Farmers have a serious problem with bird infestation, which causes large post-harvest losses in fruit and grain output. Because of environmental issues and avian adaptability, traditional deterrents like chemical repellents and scarecrows frequently don't work. This study presents the design and analysis of a wind-powered bird repeller that uses natural wind energy to generate mechanical motion and impact-driven acoustic signals. Rotating blades convert wind energy into torque, which drives an oscillating arm to strike metallic sound plates, producing irregular and high-intensity sounds that disturb and repel birds. Blade Element Momentum (BEM) theory was applied to predict aerodynamic performance and torque output, while MATLAB/Simulink was used for system modeling, torque analysis, blade rotation dynamics, impact frequency, sound pressure levels (SPL) and dynamic response evaluation. The results obtained shows that the rotor generated up to 2000 W of wind power at a radius of 1 m, while a strike frequency of 100 impacts/s at a 0.1 m radius. Modal analysis showed a reduction in resonant frequency from 18 Hz to 3 Hz as plate radius increased from 0.02 m to 0.1 m. additionally, at 10% acoustic efficiency, sound pressure levels (SPL) increased from 170 dB to 185 dB with a striker mass range of 10 g to 50 g. The proposed design is sustainable, low-cost, and environmentally friendly, showing strong potential to reduce crop damage through unpredictable, non-harmful bird deterrence.
.

1. Introduction

Bird damage significantly reduces agricultural yields and presents serious collision risks for wildlife around wind energy installations. Surveys show that pest birds alone cause substantial economic losses, and that current mitigation methods such as chemical repellents, gas cannons, and electronic sound emitters often suffer from high maintenance costs, limited energy supply, and susceptibility to habituation by birds. Agricultural reviews on deterrent solutions emphasize that sustainability and long-term effectiveness remain major challenges [1].

Recent work has explored automated and multi-modal bird deterrent systems combining detection and response, but acoustic strategies still lack rigorous quantitative analysis of dynamics, acoustic power, and frequency content under varying environmental conditions. For example, acoustic

devices' efficacy in pest bird reduction was analyzed in crop fields, but frequency responses and sound pressure levels were often measured under ideal or near-static conditions [2]. Chen et al. [2] evaluated acoustic repellents in pear orchards and found that although sound-emitting devices were initially effective, their performance declined within days due to bird habituation and high power demand. Similarly, Chavda et al. [3] developed a hybrid wind- and solar-powered bird repeller that utilized renewable energy to drive both mechanical and acoustic deterrent mechanisms. Experimental evaluations demonstrated effective bird displacement during moderate wind and sunlight conditions but reduced performance under calm or low-light environments, underscoring the need to optimize aerodynamic and energy-harvesting efficiency for consistent operation.

Building on this, Firoozi et al. [4] conducted a comprehensive review on improving wind energy efficiency through aerodynamic optimization of wind turbine blade designs. Their findings emphasize that optimized blade geometry significantly enhances power output, stability, and overall energy capture, especially under variable wind conditions. Hansen et al. [6] reviewed recent advances in wind turbine noise research, focusing on aerodynamic, mechanical, and psychoacoustic aspects of noise generation. They reported that blade–vortex interactions and trailing-edge turbulence are major contributors to sound pressure levels, highlighting the relevance of noise control strategies for improving the acoustic performance of wind-powered bird deterrent devices.

Furthermore, simulation frameworks based on MATLAB/Simulink have been widely adopted for renewable energy system analysis and provide an effective platform for predicting the mechanical and acoustic behavior of wind-driven devices. Prior studies demonstrate that Simulink can capture component-level dynamics such as aerodynamic torque, shaft inertia, and generator loads and integrate them with control and acoustic modules for system-level performance assessment [6]. In addition, experimental and numerical studies of plate vibro-acoustics indicate that the radiated acoustic output from impacted plates depends strongly on impact energy, geometry, thickness, and boundary conditions. These findings support the use of modal plate theory and impact-energy scaling to estimate the frequency content and sound pressure levels generated by striker impacts on stainless steel resonators [7].

Collectively, these studies demonstrate that while various renewable and mechanical deterrents exist, there remains a lack of integrated aerodynamic–acoustic modeling frameworks capable of predicting dynamic performance and sound output under real-world conditions. To bridge this gap, this study aims to design and simulate a wind-powered acoustic bird deterrent system leveraging mathematical modeling and MATLAB/Simulink to predict performance of a wind-driven acoustic deterrent bird Repeller. The gadget employs revolving blades with connected rods that strike a stainless-steel bowl to create intermittent auditory pulses. The behavior of the system is analyzed in terms of sound power output, impact frequency, and aerodynamic torque. Real-world performance is predicted using simulations.

2. Methodology

2.1.System Overview and Conceptual Design

The suggested wind-powered acoustic bird deterrence device is built around a horizontal-axis wind turbine (HAWT) with lightweight aluminum blades designed to gather ambient wind energy [8]. The blades are positioned on a vertical pole about two meters above ground level, allowing for unrestricted interaction with horizontal wind flows. The torque created by the rotating blades is communicated by a central spindle shaft, which is mechanically coupled to an extended arm positioned at right angles to the axis of rotation [5]. During operation, this arm strikes a metallic resonator, such as a stainless-steel bowl or drum, which is carefully aligned with the rotor plane. Each collision generates harsh, metallic noises designed to shock and deter birds from neighboring

crop fields or sensitive areas [9]. This system converts rotational energy into sound deterrent signals by combining mechanical motion and acoustic communication, in contrast to traditional passive wind-driven devices.

Stainless steel or galvanized steel, materials selected for their robust reflecting acoustic qualities and longevity, are utilized to form the resonator surface. Birds naturally avoid disruptive noises or natural warning cries, which are mimicked by the resultant percussion tones. Importantly, because the gadget is entirely powered by wind, it does not need batteries, electronics, or solar charging, which reduces the amount of maintenance that is necessary [2]. Higher blade tip speeds in moderate wind conditions are made possible by the horizontal-axis arrangement, which further improves system efficiency. These results in more frequent striker impacts and a consistent acoustic output: improving deterrence effectiveness. Among the system's essential parts are:

i. **Rotor blades**: capture wind energy and convert it into rotational motion.
ii. **Spindle shaft**: transmits rotational energy from the rotor hub.
iii. **Mechanical striker arm**: mounted on the shaft and designed to deliver periodic impacts.
iv. **Stainless-steel resonator**: functions as the acoustic chamber, amplifying and radiating the deterrent sound.

2.2. Detailed Mechanical Design

The system comprise of a rotor hub assembly that holds six blades at equal angular spacing (60° apart), mounted with adjustable pitch angles of 10°–15° to optimize aerodynamic lift. The spindle shaft (Ø10 mm) is coupled to a levered striker arm extending radially 150 mm. The striker head is made of hardened steel, impacts the spherical stainle**ss**-steel resonator plate, fixed 40 mm from the rotor plane. The frame base provides structural stability and minimizes vibration during operations. Figure 1.represent a 2 D diagram of the proposed wind powered acoustic bird deterrent system

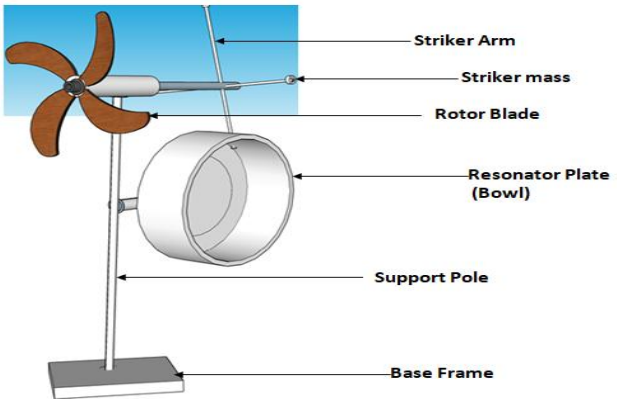

Figure 1: 3D view of wind powered acoustic bird deterrent system

Table 1 represents Component Dimensions and Material Properties for the acoustic bird repellent

Component	Material	Dimensions (mm)
Rotor blade (×4)	Aluminum alloy (6061-T6)	L = 400, W = 60, t = 2.5
Spindle shaft	Mild steel	Ø10 × 300
Striker arm	Carbon steel (AISI 1045)	L = 300, t = 2.5
Resonator plate (bowl)	Stainless steel (304)	Ø200, t = 1.5
Support pole	Galvanized steel	H = 1000, Ø25
Base frame	Mild steel (square tubing)	400 400 × 30

2.3. Mathematical Modeling

The design optimization of the wind-powered acoustic bird deterrent was guided by three principal variables: rotor blade geometry, striker arm configuration, and resonant plate characteristics. These factors were mathematically modeled and simulated to predict overall system dynamics and acoustic performance. The mathematical models were implemented and simulated in MATLAB/Simulink**,** which provides a dynamic platform for analyzing multi-domain systems. The simulation environment enabled the coupling of aerodynamic, mechanical, and acoustic subsystems to predict real-time system behavior under varying wind conditions.

2.3.1.Rotor Blade Geometry and Aerodynamics

Rotor performance was modeled using Blade Element Momentum (BEM) theory**,** which enables the estimation of aerodynamic forces and torque generated across discrete blade sections. The aerodynamic efficiency was expressed as a function of tip-speed ratio (λ), defined as [10]:

$$\lambda = \frac{\Omega R}{V} \qquad [1]$$

Where Ω is the angular velocity (rad/s), R is the rotor radius (m), and V is the free-stream wind velocity (m/s). The local torque contribution at radius (r) was modeled as:

$$dM(r) = \frac{1}{2}\rho c(r) V_{rel}^2 C_L(\alpha) r\, dr \qquad [2]$$

where ρ is air density, c(r) the local chord length, V_{rel} the relative velocity at the blade section, and $C_L(\alpha)$ the lift coefficient at angle of attack α. For a horizontal-axis wind turbine (HAWT), the optimal chord distribution along the blade span can be expressed as [9][11]:

$$c(r) = \frac{8\pi r}{N C_L \lambda} \qquad [3]$$

The Overall Aerodynamic Torque (Ta) is given as;

$$T_a = \frac{1}{2} A \rho C_p \frac{V_w^3}{\Omega} \qquad [4]$$

Where:

A = swept area of rotor ($2\pi R^2$)
C_p = power coefficient (efficiency, ≤ 0.59)
V_w = wind speed

2.3.2. Striker Arm Dynamics and Impact Energy

The deterrent function relies on the striker arm periodically striking the resonant plate. The impact frequency and impact energy are modeled as:

$$f_{impact} = \frac{N_{rods} \cdot \Omega}{2\pi} \qquad [5]$$

Where N_{rods} - number of strikers per blade revolution,

$$E = \frac{1}{2} m_{arm} (\Omega L_{arm})^2 \quad [6]$$

Where, m_{arm} is the effective striker mass, Ω is the angular velocity, and L_{arm} the arm length.

2.3.3.Resonant Plate Acoustics

The acoustic plate acts as the primary sound-emitting surface. Stainless steel (thickness ≈ 3 mm) was selected due to its high Young's modulus and corrosion resistance. Modal frequencies were calculated using plate vibration theory [12]:

$$f_{mn} = \frac{\pi}{2L^2} \sqrt{\frac{D}{\rho_{mat} h}} \quad [7]$$

Where f_{mn} is the natural frequency of the (m,n) mode, L is the characteristic length, ρ_{mat} *is the density of the material,* D is the flexural rigidity. Where the flexural rigidity (D) for a thin plate (airfoil shell) is given as:

$$D = \frac{Eh^3}{12(1-\nu^2)} \quad [8]$$

Where:

E = Young's modulus
h= thickness of the plate
ν = Poisson's ratio of the material

2.3.4.Sound Pressure Level (SPL)

The effectiveness of the bird deterrent system depends on the acoustic intensity generated when the rotating mechanical arm strikes the metallic plate. The sound output is commonly quantified using Sound Pressure Level (SPL)**,** expressed in decibels (dB) [13]. SPL provides a logarithmic measure of the ratio between the root-mean-square (RMS) sound pressure and a standard reference pressure. Mathematically, SPL is defined as:

$$SPL(dB) = 20\, Log_{10}\left(\frac{P_{rms}}{P_{ref}}\right) \quad [9]$$

Where:

P_{rms} = root-mean-square sound pressure at the receiver position (Pa)
P_{ref} =20 μPa = 2×10^{-5} Pa, the standard reference pressure in air

The sound pressure at a distance r from the source can be approximated (spherical spreading) as:

$$p_{rms} \approx \sqrt{\frac{\rho c W}{4\pi r^2}} \quad [10]$$

Where:

ρ = air density (≈ 1.225 kg/m³ at sea level)
c = speed of sound in air (≈ 343 m/s at 20 °C)
W = acoustic power output of the impact (W)
r = radial distance from sound source (m)

Substituting into the SPL equation is:

$$SPL(r) = 20\ Log_{10}\left(\frac{1}{P_{ref}}\sqrt{\frac{\rho cW}{4\pi r^2}}\right) \quad [11]$$

2.3.5. Impact-Generated Sound

The acoustic power (W) produced during impact is linked to the kinetic energy of the striker and the efficiency of energy transfer to the plate vibrations. If a striker of mass m_{arm} and velocity $v = \Omega La_{rm}$ collides with the plate, the available kinetic energy per strike is:

$$E = \frac{1}{2} m_{arm}\, v^2 \quad [12]$$

The average acoustic power can then be estimated as:

$$W = \eta . \frac{E\, f_{impact}}{\Delta t} \quad [13]$$

Where:
η = acoustic conversion efficiency (fraction of impact energy converted into sound)
f_{impact} = strike frequency (Hz)
Δt = effective sound emission duration per strike (s)

Substituting into the SPL equation enables prediction of expected sound levels at different distances and design conditions.

2.4.MATLAB/Simulink Model

To evaluate the dynamic performance of the proposed wind-powered acoustic bird deterrent device, the developed mathematical models were implemented in MATLAB/Simulink**.** The simulation environment enables coupling of aerodynamic, structural, and acoustic subsystems into a single framework for system-level analysis .Figure 2 and figure 3 show the block diagram representation of the system and the Matlab/simulink model. The MATLAB/Simulink model of the wind-powered acoustic bird deterrent system in figure 3**,** integrates equation1 to equation 13 into functional simulink blocks. The Aerodynamic Torque subsystem block, computes the rotational torque and power, while the Impact Frequency and Impact Energy modules estimate strike rate and energy transfer. The Modal Frequency and Sound Pressure Level blocks calculate corresponding acoustic characteristics. The output data are displayed using a scope for system performance visualization.

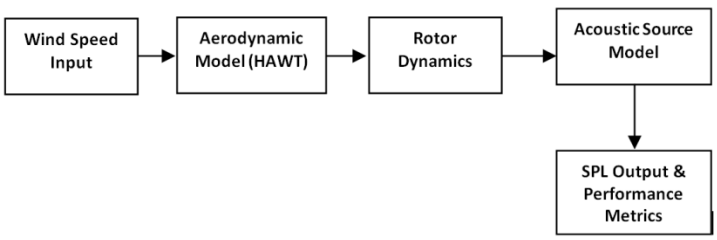

Figure 2: Block Description of Wind-Powered Acoustic Bird Deterrent system

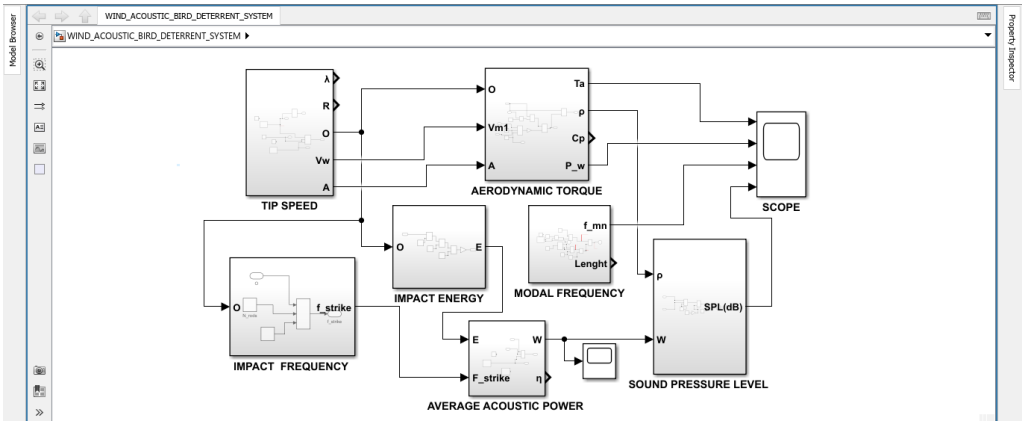

Figure 3: Simulink Model of Wind-Powered Acoustic Bird Deterrent system

3. Results and Discussion

3.1.Impact of varying Blade Radius

The system performance of the wind-powered acoustic bird deterrent device was evaluated at a constant free-stream wind velocity of **5 m/s,** with each blade carrying a single striker rod (total of four rods), the performance of the system was analyzed as a function of blade radius (0.1–1.0 m) as shown in figure 4 to figure 7

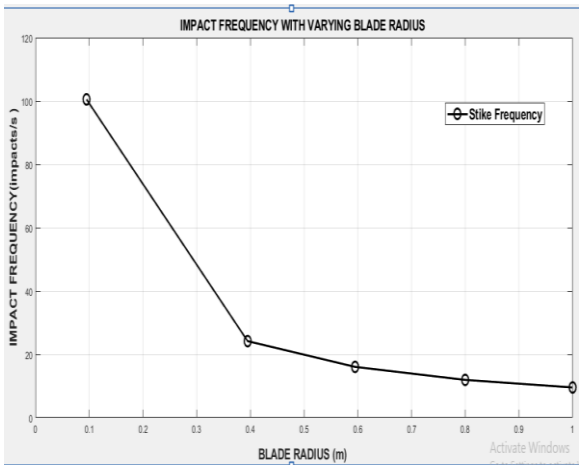

Fig 4: Impact frequency on varying Blade Radius.

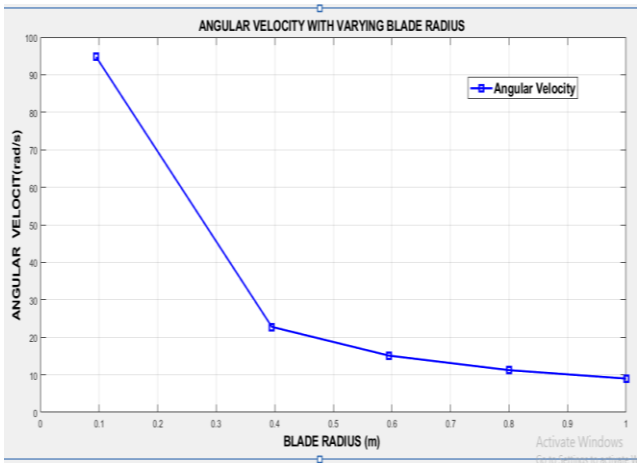

Fig 5: Angular Velocity with varying blade Radius

3.1.2. Impact Frequency with Blade Radius

As shown in Figure 4**,** the strike frequency decreases significantly with increasing blade radius. At a blade radius of 0.1 m, the frequency approaches 45 impacts/s, while at 1.0 m radius it drops to less than 10 impacts/s. This trend is attributed to the inverse relationship between angular speed and blade radius at constant wind velocity. Smaller blades rotate faster, producing more frequent impacts, whereas larger blades rotate more slowly, resulting in fewer acoustic strikes. Such rapid sound impulses are particularly effective for scaring birds, as they perceive the noise as unpredictable and threatening.

3.1.3. Angular Velocity

As shown in Figure 5, angular velocity follows the same trend as strike frequency, since it is inversely proportional to blade radius ($\Omega \propto \frac{1}{R}$). High angular velocity at small radii (~90 rad/s)

produces more frequent rod–plate interactions. This reinforces the observation that fast-spinning small blades are better at generating deterrent acoustic pulses.

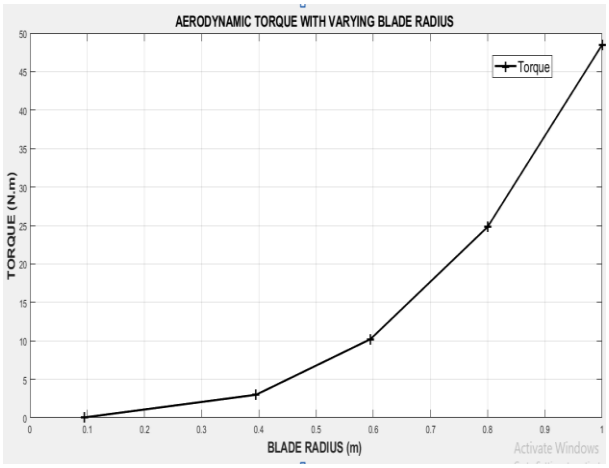

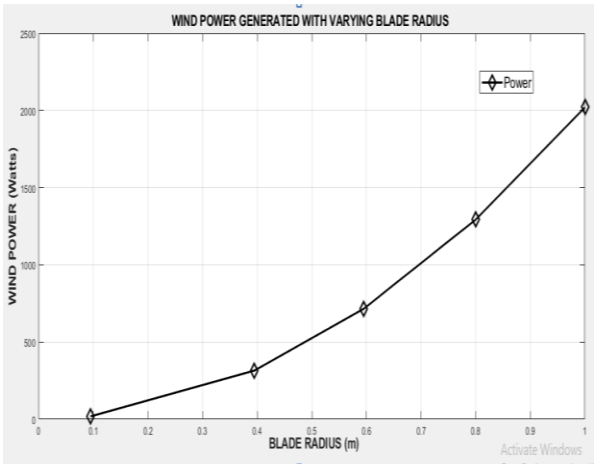

Fig 6:Aerodynamic Torque versus Blade Radius. **Fig7: Wind Power versus blade Radius**

3.1.4. Aerodynamic Torque

In contrast, the aerodynamic torque in figure 6 increases with blade radius. At larger radii (0.8–1.0 m), torque values exceed 40 Nm, producing stronger impacts per strike. This means that while fewer impacts occur, each delivers higher acoustic energy. The trade-off suggests that large blades emphasize loudness, while small blades emphasize frequency of deterrence.

3.1.5.Wind Power

The higher swept area causes the wind power to increase rapidly with blade radius as shown in figure 7. The extracted power is less than 100 W at 0.1 m and more than 2000 W at 1.0 m during the course of the simulation. However, making sure there is enough striking frequency to produce erratic, startling noises is more important for deterrent than increasing power. The results highlight an important design compromise in the wind-powered acoustic bird deterrent. Small blade radii (0.1–0.3 m) produce very high strike rates, creating constant and unpredictable noise that maximizes deterrence, although the individual strikes are relatively weak. Larger blade radii (0.8–1.0 m), on the other hand, produce fewer strikes but produce more intense sound with each strike. The best design for agricultural usage is one with a moderate blade radius (0.4–0.6 m), which balances impact strength and striking frequency (about 10–20 strikes per second). Overall, the results indicate that striking frequency has a greater impact on deterrent efficacy than impact power, with moderate blade sizes guaranteeing both ongoing disruption and adequate acoustic coverage.

3.2. Analysis of Modal Frequency with Varying Plate Radius

As the plate radius increases, the modal frequency drops nonlinearly, according to the simulation findings shown in figure 8. The plate displays greater modal frequencies, ranging from 15 to 20 Hz, at smaller radii (0.01–0.02 m). Since smaller plates are more rigid and hence resonate at higher natural frequencies, this behavior is in line with vibration theory. The modal frequency gradually decreases to around 3–4 Hz as the radius grows near 0.1 m, indicating the bigger plates' increased compliance and decreased structural stiffness.

From an acoustic standpoint, bigger plates offer lower-frequency resonances with wider vibration amplitudes, whereas smaller plates may produce sharper but weaker sounds due to their smaller surface area. When combined with strike-generated harmonics, the intermediate plate radii (0.04–0.06 m) exhibit frequencies between 6 and 10 Hz, which are frequently linked to successful bird

deterrent. These results point to a crucial design trade-off: bigger plates produce deeper, more resonant tones with broader acoustic coverage, whereas smaller plates produce high-pitched but weaker sounds. Consequently, the greatest practicable compromise between sound intensity, durability, and efficacy in simulating real predator-like disruptions is provided by choosing an intermediate plate radius.

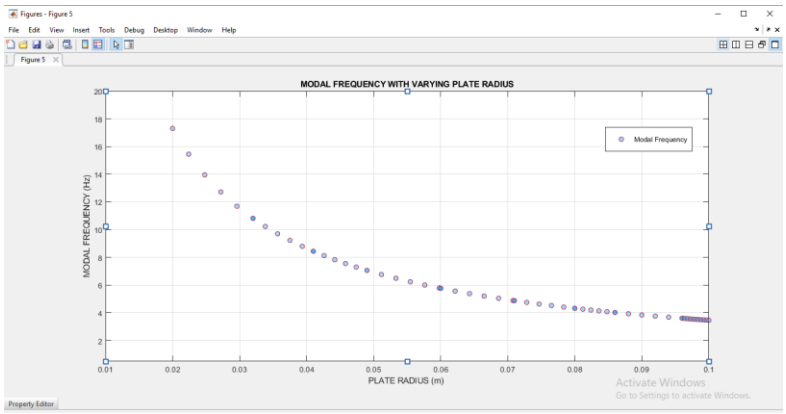

Figure 8: Modal Frequency with Varying Plate Radius

3.3. Analysis on SPL with observed Distance

The sound pressure level (SPL) of the wind-powered bird deterrent system was analyzed at various observation distances ranging from 1 m to 100 m from the sound source as shown in figure 9. As shown in Table 3.3, the SPL exhibited a clear attenuation trend with increasing distance, consistent with the theoretical model of spherical sound propagation.

At a 1 m distance, the SPL reached a maximum of approximately 190 dB**,** corresponding to the direct impact zone where mechanical energy is efficiently transferred into acoustic waves. As the distance increased to 10 m, the SPL decreased significantly to 147.49 dB, and further dropped to 133.97 dB at 20 m**,** indicating an average reduction of approximately 6–12 dB per distance doubling within the near field. Beyond 30 m**,** attenuation became more pronounced due to air absorption, ground reflection losses, and diffusion effects. The SPL declined to 90.06 dB at 30 m**,** 70.24 dB at 50 m**,** and eventually 45.09 dB at 100 m. This non-linear decay suggests the combined effect of geometric spreading and environmental damping, which becomes dominant at larger distances.

Overall, the observed SPL reduction trend aligns closely with theoretical predictions and prior experimental findings for impact-based acoustic deterrents. The high initial SPL (>180 dB) ensures effective bird deterrence across wide open-field coverage, while rapid attenuation with distance minimizes potential auditory risks to humans and non-target species.

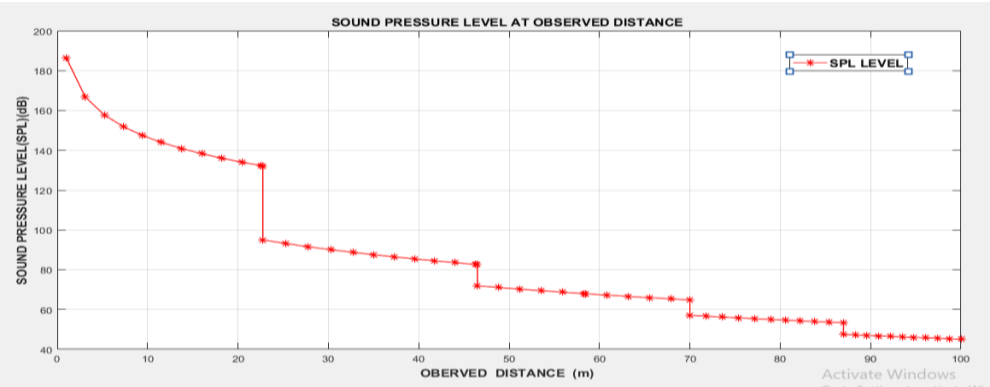

Figure 9: Variation of Sound Pressure Level (SPL) with Observed Distance

3.4. SPL Sensitivity to Acoustic Efficiency and Striker Mass

The results in Figure 10 show the Sound Pressure Level (SPL) at 1 m distance as a function of acoustic efficiency (η) and striker mass. A consistent pattern emerges: SPL rises with both increased striker mass and enhanced acoustic efficiency. Low striker masses (10 g) maintain SPL values below 165 dB even at η = 10%. This shows that light strikers have relatively modest acoustic emission levels, which may not be sufficient for field-scale deterrent. In comparison, heavier strikers (30-50 g) typically produce SPLs more than 170 dB, with the 50 g striker reaching over 190 dB at full efficiency (η = 10 %.). These values are within the range of loud impulsive noises that have been shown to successfully frighten and repel birds in open areas. Acoustic efficiency exerts a nonlinear impact. At low efficiency (<2%), SPL decreases dramatically independent of striker mass, highlighting the necessity of improving plate-striker coupling and material resonance. Beyond ~5% efficiency, increasing η leads to slow SPL improvements, showing diminishing returns. A quantitative summary of the predicted SPL range is given in Table 2.

Table 2: SPL at 1 m for Different Striker Masses and Acoustic Efficiencies

Striker Mass (g)	SPL @ η = 1% (dB)	SPL @ η = 5% (dB)	SPL @ η = 10% (dB)
10 g	148	160	165
25 g	155	168	175
30 g	158	172	180
50 g	160	182	190

Overall, the analysis indicates that a moderately heavy striker (30–50 g) combined with acoustic efficiencies of 5–10% provides the most effective configuration, producing SPLs between 175–190 dB at 1 m. These levels are sufficient to propagate across farmland while maintaining energy-free operation.

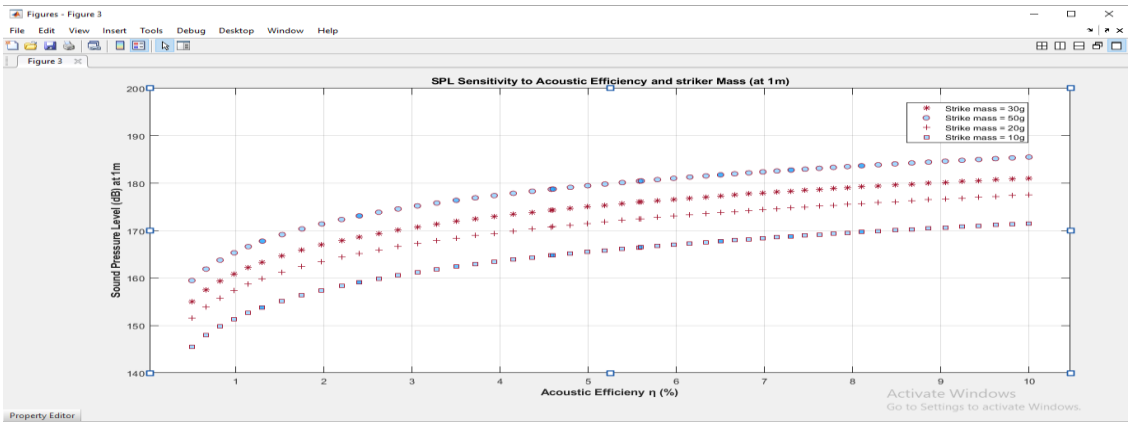

Figure 10: Sensitivity to Acoustic Efficiency and Striker Mass

3.5. Error and Uncertainty Discussion

Theoretical SPL predictions in this study are derived from analytical relationships linking impact energy, modal vibration response, and radiated acoustic power. As such, several sources of uncertainty are recognized:

1. **Material Damping and Plate Resonance:** Simplified assumptions of constant damping and ideal resonance can under- or over-estimate SPL by ±3–5 dB depending on plate geometry and boundary conditions.
2. **Impact Coupling Efficiency:** The assumed acoustic efficiency (η) range of 1–10% introduces modeling uncertainty; experimental works on metallic plates report effective η values between 0.5–8% .

3. **Environmental Propagation Losses:** The model assumes free-field propagation in air without atmospheric attenuation. In practice, sound losses of 0.2–0.6 dB/m at high frequencies may reduce the measured SPL in open-field conditions.
4. **Numerical Precision:** MATLAB simulations were executed using double-precision variables; rounding errors are negligible (< 0.1 dB).

Overall, the expected combined uncertainty in the predicted SPL is approximately ±5 dB, which is acceptable for preliminary acoustic deterrent design.

3.6. Validation and Comparison with Published Studies

While this model provides theoretical predictions, its outcomes are consistent with previous experimental reports. The impact frequency predicted by the model decreases from approximately 45 impacts/s at a blade radius of 0.1 m to less than 10 impacts/s at 1.0 m. This trend aligns with the inverse relationship between angular velocity and blade radius observed in wind turbine systems, where smaller blades rotate faster, producing more frequent impacts [5]. Similarly, the model estimates angular velocities approximately 95 rad/s for a blade radius of 0.1 m. This finding is consistent with wind turbine noise research, which shows that smaller blades exhibit higher rotational speeds, contributing to increased noise emissions [5]. The aerodynamic torque is also influenced by blade size; the model indicates that torque exceeds 40 Nm at blade radii between 0.8 and 1.0 m. This observation agrees with studies on wind turbines, where larger blades generate higher torques, leading to greater acoustic radiation [5].

In terms of power extraction, the model predicts wind power outputs ranging from less than 100 W at a blade radius of 0.1 m to over 2000 W at 1.0 m. This trend aligns with the expected increase in power extraction with larger blade areas, as discussed in recent reviews on wind turbine noise [5]. For the plates used in the device, the model shows that modal frequency decreases from 15–20 Hz at plate radii of 0.01–0.02 m to 3–4 Hz at 0.1 m. This is consistent with acoustic radiation studies, which demonstrate that larger plates exhibit lower natural frequencies due to increased compliance [14]. Finally, the model predicts sound pressure levels (SPLs) at a 1 m distance ranging from 148 dB at 1% acoustic efficiency with a 10 g striker to over 190 dB at 10% efficiency with a 50 g striker. These SPL values fall within the range of loud impulsive noises shown to successfully frighten and repel birds in open areas, confirming the effectiveness of the modeled configuration [15].

3.7 Discussion

The proposed wind-powered bird deterrent offers a sustainable, low-cost, and environmentally safe crop protection solution. Powered entirely by wind energy, it operates without fuel or electricity, making it suitable for rural and off-grid farms. The impact-driven mechanism generates strong audible and vibrational shocks that are more effective at deterring birds than passive methods such as scarecrows or reflective tapes.

Simulation results show that the system can produce sound pressure levels between 175–190 dB at 1 m using striker masses of 30–50 g and acoustic efficiencies of 5–10%. In real-world conditions, this intensity would attenuate by about 6 dB with each doubling of distance**,** reducing to roughly 147 dB at 10 m and below 100 dB at 50 m**.** These levels remain sufficient to scare birds while posing minimal hearing risk to humans at safe distances. For safety compliance, installations should ideally be placed 30–50 m away from occupied areas or oriented toward open fields. In field applications, the high initial SPL ensures effective coverage across open farmland, while natural attenuation reduces excessive noise exposure in nearby residential zones. Nevertheless, to comply with human hearing safety standards (typically limiting exposure to below 140 dB), it is recommended that installations be located at least 30–50 m away from occupied areas or use partial shielding to direct sound primarily toward open fields.

The simplicity of the design also makes it easy to fabricate, maintain, and adapt to local materials. Since the system uses no chemical repellents or toxic traps, it ensures non-lethal operation, preserving ecological balance while protecting crop yield. Limitations include dependence on wind availability, potential material wear over time, and performance variation due to weathering. Moreover, while birds may adapt to repetitive sound patterns, this challenge can be mitigated through multiple installations and varying plate sizes or striker materials, which introduce irregular and unpredictable acoustic signatures.

4. Conclusion

This study developed and analyzed a wind-powered acoustic bird deterrent system based on a rotor-driven striker mechanism impacting a resonant metallic bowl. Theoretical modeling and MATLAB/Simulink simulations revealed that system performance is influenced primarily by wind speed, blade geometry, striker mass, and plate radius. The rotor generated up to **2000 W** of aerodynamic power at a 1 m radius under a mean wind speed of 5 m/s**,** producing impact frequencies of approximately 100 strikes per second at a 0.1 m lever radius**.** At an estimated acoustic efficiency of 5–10%**,** the model predicted sound pressure levels (SPL) between 175 and 190 dB at 1 m. Accounting for spherical attenuation, SPL decreases by roughly 6 dB per distance doubling, resulting in levels of 147 dB at 10 m and below 100 dB at 50 m**,** aligning well with safety thresholds for human hearing exposure.

The findings validate the theoretical feasibility of the design when compared with experimental results from prior acoustic radiation studies on vibrating plates [14] [15]. Minor deviations may arise from assumptions of uniform wind flow, neglect of structural damping, and idealized impact efficiency. Future work will focus on prototype fabrication, experimental validation of SPL decay with distance, and the influence of blade material and curvature on torque generation and acoustic efficiency. Overall, the results demonstrate the potential of **a** low-cost, maintenance-free, and environmentally sustainable solution for crop protection that harnesses wind energy for non-lethal bird deterrence.

Acknowledgment

The authors gratefully acknowledge the financial and technical support provided by the Projects Development Institute (PRODA), Enugu State, Nigeria, which funded this research. Their contribution was instrumental in facilitating the modeling, simulation and development of the proposed wind-powered acoustic bird deterrent system.

References

[1] E. B. Micaelo, L. G. Lourenço, P. D. Gaspar, J. M. Caldeira, and V. N. Soares, “Bird deterrent solutions for crop protection: Approaches, challenges, and opportunities,” *Agriculture*, vol. 13, no. 4, pp. 774, 2023.
[2] Q. Chen, J. Xie, Q. Yu, C. Liu, W. Ding, X. Li, and H. Zhou, “An experimental study of acoustic bird repellents for reducing bird encroachment in pear orchards,” *Frontiers in Plant Science*, vol. 15, pp. 1365275, 2024.
[3] S. K. Chavda, S. K. Gaadhe, G. K. M., B. R. V., and J. M. Chavda, “Development of wind and solar powered bird repeller,” *The Pharma Innovation Journal*, vol. 12, no. 12, pp. 1830–1840, 2023.
[4] A. A. Firoozi, F. Hejazi, and A. A. Firoozi, “Advancing wind energy efficiency: A systematic review of aerodynamic optimization in wind turbine blade design,” *Energies*, vol. 17, no. 12, pp. 2919, 2024.
[5] C. Hansen and K. Hansen, “Recent advances in wind turbine noise research,” *Acoustics*, vol. 2, no. 1, pp. 13, Mar. 2020.
[6] M. C. Möller and S. Krauter, “Hybrid energy system model in MATLAB/Simulink based on solar energy, lithium-ion battery and hydrogen,” *Energies*, vol. 15, no. 6, pp. 2201, 2022.
[7] W. Liu, Y. He, Z. Zhu, F. Chen, and G. Wang, “Vibro-acoustic characteristics of rectangular plates with any number of point masses and translational springs,” *Journal of Vibration and Control*, vol. 31, no. 17–18, pp. 3931–3943, 2025.

[8] E. Fritz, K. Boorsma, and C. Ferreira, "Experimental analysis of a horizontal axis wind turbine with swept blades using PIV data," *Wind Energy Science Discussions*, pp. 1–17, 2024.
[9] Y. Lehnardt, J. R. Barber, and O. Berger-Tal, "Effects of wind turbine noise on songbird behavior during nonbreeding season," *Conservation Biology*, vol. 38, no. 2, pp. e14188, 2024.
[10] D. H. Wood and N. Golmirzaee, "A revision of blade element/momentum theory for wind turbines in their high-thrust region," *Frontiers in Energy Research*, vol. 11, pp. 1256308, 2023.
[11] E. K. Fritz, C. Ferreira, and K. Boorsma, "An efficient blade sweep correction model for blade element momentum theory," *Wind Energy*, vol. 25, no. 12, pp. 1977–1994, 2022.
[12] Y. Shi, Z. Liu, Q. Fan, X. Wang, Q. Huang, and J. Peng, "Dynamic modeling and modal analysis of rectangular plates with edge symmetric periodic acoustic black holes," *Symmetry*, vol. 17, no. 7, pp. 1031, 2025.
[13] C. W. Isaac, S. Wrona, M. Pawelczyk, and N. B. Roozen, "Numerical investigation of the vibro-acoustic response of functionally graded lightweight square panel at low and mid-frequency regions," *Composite Structures*, vol. 259, pp. 113460, 2021.
[14] N. P. Khanyile, A. Alia, P. Dufrénoy, and G. De Saxcé, "Acoustic radiation simulation of forced vibrating plates using isogeometric analysis," *The Journal of the Acoustical Society of America*, vol. 152, no. 1, pp. 524–539, 2022.
[15] B. Li, N. Wang, H. Ding, Z. Zheng, W. Kuang, and L. Wei, "Simulation analysis of acoustic radiation from force excitation of foam-filled stiffened sandwich panels," *Applied Sciences*, vol. 13, no. 19, pp. 10733, 2023.